

# Flow-based assembly of nucleic acid-loaded polymer nanoparticles

 Zeyan Xu<sup>A</sup>, Joshua McCarroll<sup>B,C,D</sup> and Martina H. Stenzel<sup>A,D,\*</sup> 

For full list of author affiliations and declarations see end of paper

**\*Correspondence to:**

 Martina H. Stenzel  
 School of Chemistry, University of New South Wales, Sydney, NSW 2052, Australia  
 Email: [m.stenzel@unsw.edu.au](mailto:m.stenzel@unsw.edu.au)
**Handling Editor:**

Curt Wentrup

**Received:** 20 June 2023

**Accepted:** 8 August 2023

**Published:** 29 August 2023

**Cite this:**

 Xu Z *et al.* (2023)  
*Australian Journal of Chemistry*  
**76**(11), 731–745. doi:[10.1071/CH23116](https://doi.org/10.1071/CH23116)

© 2023 The Author(s) (or their employer(s)). Published by CSIRO Publishing.

 This is an open access article distributed under the Creative Commons Attribution-NonCommercial-NoDerivatives 4.0 International License ([CC BY-NC-ND](https://creativecommons.org/licenses/by-nc-nd/4.0/))

OPEN ACCESS

**ABSTRACT**

Since the development of messenger RNA (mRNA)-based SARS-CoV-2 (COVID-19) vaccines, there is increased public awareness of the importance of nanoparticles, in this case lipid nanoparticles, to ensure safe delivery of an active compound. To ensure the formation of high-quality nanoparticles with reproducible results, these lipid nanoparticles are assembled with the nucleic acid drug using flow-based devices. Although flow assembly using lipid nanoparticles for nucleic acid delivery is well described in the literature, only a few examples use polymers. This is surprising because the field of polymers for nucleic acid delivery is substantial as hundreds of polymers for nucleic acid delivery have been reported in the literature. In this review, we discuss several aspects of flow-based assembly of nucleic acid-loaded polymer nanoparticles. Initially, we introduce the concept of chip-based or capillary-based systems that can be either used as single-phase or multiphase systems. Initially, researchers have to choose the type of mixing, which can be active or passive. The type of flow, laminar or turbulent, also significantly affects the quality of the nanoparticles. We then present the type of polymers that have so far been assembled with mRNA, small interfering RNA (siRNA) or plasmid DNA (pDNA) using flow devices. We discuss effects such as flow rate, concentration and polymer lengths on the outcome. To conclude, we highlight how flow assembly is an excellent way to generate well-defined nanoparticles including polyplexes in a reproducible manner.

**Keywords:** DNA, drug delivery, flow assembly, gene therapy, microfluidics, nanomedicine, polymers, RNA, self-assembly.

**Introduction**

Nanoparticles are widely used for drug delivery.<sup>1</sup> From initial concepts, this field has now matured and many drug-loaded nanoparticles have now entered clinical trials or are available on the market.<sup>2,3</sup> The impact of nanoparticles in the medical field became evident during the SARS-CoV-2 (COVID-19) pandemic when lipid nanoparticles made it possible to deliver the mRNA (messenger ribonucleic acid) vaccines, which cannot be administered otherwise.<sup>4</sup> Although nanoparticles can enhance the delivery of most drugs, no other class of drugs benefits from nanoparticles as much as nucleic acid-based therapeutics since nanoparticles can protect the drug while enhancing circulation time and cellular uptake.<sup>5,6</sup> Lipid nanoparticles are a great success in vaccine delivery; however, other diseases require more tailor-made nanoparticle solutions and therefore this field is still evolving. When new nanoparticles are developed,<sup>7</sup> researchers usually consider the interface between the nanoparticle and the biological environment as parameters such as surface chemistry, type of nanoparticles, size and shape and other physical properties influence the fate of the nanoparticle.<sup>8–10</sup>

Size is important in drug delivery.<sup>11</sup> Smaller nanoparticles usually have longer circulation times in the blood stream as demonstrated with gold nanoparticles between 10 and 100 nm.<sup>12,13</sup> Although reducing the size can be beneficial, nanoparticles below 10 nm are readily removed by renal filtration.<sup>14</sup> Meanwhile, large particles above 100 nm can be quickly cleared by the mononuclear phagocytic system (MPS)<sup>15,16</sup> or they accumulate in

the liver and spleen.<sup>17</sup> There are size sweet spots when it comes to tumour extravasation and penetration. Smaller nanoparticles, well below 50 nm, penetrate deeper into tumours,<sup>13,18</sup> whereas extravasation, which relies on translocation through fenestration in the tumour vasculature, is often more efficient with nanoparticles above 50 nm in size. It is therefore evident that size plays a pivotal role in drug delivery, but there is also a paradox as each delivery step – circulation, extravasation, penetration and cell uptake – favours different nanoparticle sizes.<sup>19</sup>

It is therefore essential not only to determine the average size of nanoparticles, but also evaluate the particle size distribution because a broad size distribution would result in unexpected biodistributions as the smaller fraction behaves differently to the larger fraction of the sample. There is often little attention to size distribution but reports on polydispersity indices (PDIs) measured using dynamic light scattering (DLS) of more than 0.2 are common. PDI is defined as the square of the standard deviation over the mean size, which means that a mean size of 50 nm and a PDI value of 0.2 has a standard deviation of 22 nm! Broad nanoparticle distributions are typically obtained when nanoparticles are prepared by hand in the laboratory, and, despite the use of syringe pumps and other control measures, broad distributions are ingrained in the preparation techniques. This is evident when mixing cationic polymers with negatively charged therapeutic nucleic acids. A plethora of different cationic polymers have been condensed with mRNA, plasmid DNA (pDNA), antisense oligonucleotides (ASOs) and similar therapeutics by electrostatic interaction.<sup>5</sup> In a typical experiment, the polymer is added to the nucleic acid or vice versa, which means that during the addition process, the composition of the solution changes, which changes the nanoparticle properties in the next step (Fig. 1). These heterogeneities in this bulk mixing process can then result in a broad distribution of nanoparticle sizes and compositions. Electrostatic interactions are fairly strong

and there is limited opportunity for rearrangement once the polyplex has been formed, in particular when the polymer or the therapeutic nucleic acids are large. PDI values are often not reported, but if they are, they are typically above 0.2.<sup>20–23</sup> If we carefully scrutinise our own work, we find that PDIs are seldomly below 0.2 and, at times, extensive filtering is required to narrow the particle size distribution, which can have its own problems.<sup>22–25</sup> Polyplex formation (often also called coacervate or polyion complex formation) is not only associated with a lack of uniformity, but also with challenges in reproducing nanoparticle formation. In the present review, we summarise the approaches to well-defined nucleic acid-loaded nanoparticles using flow-based devices that can serve as laboratory and industry-based assembly lines and provide nanoparticles of a certain size in a reliable manner. The focus here will be on polymers or dendrimers as the multitude of charges on the drug carrier make it particularly difficult to generate nanoparticles with small size distributions.<sup>5</sup>

## Flow-based nanoparticle preparation devices

Low reproducibility of nanoparticle preparation, high polydispersity and a lack of avenues to scale up the process to the kilogram scale were identified as challenges that hamper nanomedicine development.<sup>26</sup> The lack of reproducibility and the urgently needed high throughput were already a subject of discussion when the field of gene delivery was established. Early devices include a system that combined two syringes that were able to mix two solutions, one with DNA and the other with lipoplex, at a controlled rate. The PLEXER was able to produce particles of ~300 nm in a reproducible manner independently of the operator.<sup>27</sup> The underpinning idea was refined over the next decade and the synthesis of lipid nanoparticles loaded with nucleic acid drugs can now be carried out at a large scale,<sup>28</sup> exemplified by mRNA COVID-19 vaccines.<sup>29</sup>

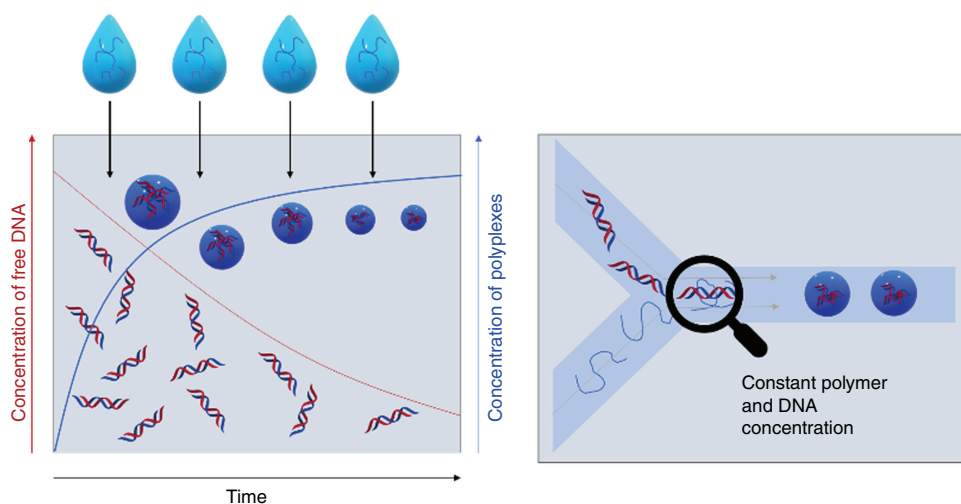


**Fig. 1.** Comparison of bulk mixing (left) and flow mixing (right) of nucleic acid and polymers. In bulk mixing, the polymer is continuously added to the solution and the amount of free nucleic acid therefore changes over time. The ratio of free DNA and polymer changes over time, and therefore the composition of the polyplexes. In flow mixing, the concentration of nucleic acid and polymer remains constant over the course of mixing.

## Chip-based and capillary-based flow devices

There are typically two types of flow devices, chip-based or capillary-based, with the commonality that two or more solutions are quickly combined.<sup>28</sup> Chip-based systems are prepared from silicon, glass or occasionally polymer and they have all functions – solution combination, mixing and equilibrium line – integrated in one device.<sup>30</sup> The channels are often square, owing to the preparation technique, with channel diameters of less than 1000  $\mu\text{m}$ . Glass-based devices are the most robust as they can withstand organic solvents and high temperature, but they are usually more expensive and fragile. In the field of nucleic acid delivery where ambient temperatures and aqueous systems are used, cheaper polymer and silicone-derived microfluidic systems can be used. Capillary-based systems are commonly assembled from tubing made for example from Teflon and a mixer that can be made from a different material. The tubing diameter is often larger than that found in microfluidic devices although there are no limitations. The most famous example is the flash nanoprecipitation system by Johnson and Prud'homme who reported

their system first in this journal in 2003.<sup>31</sup> The central part is the design of the mixer that enables rapid combination of all solutions (Fig. 2).<sup>32</sup> This system later became the foundation for the production of the COVID-19 vaccine.

## Single-phase flow system

### Active and passive mixing

The central focus in flow-based devices is the development of suitable mixing approaches. Mixing of the solutions can either be achieved by active mixing or passive means (Fig. 3).<sup>33</sup> Active mixing requires the integration of an externally controlled mixer such as acoustic, ultrasonic, thermal or dielectrophoretic force actuation, pressure perpetuation or electromagnetic micromixer.<sup>34</sup> The mixer can also be integrated in the design, as demonstrated by a design that uses an in-line rotating impeller to mix solutions.<sup>35</sup>

More commonly used in polymer laboratories, however, is passive mixing as many devices are commercially available,

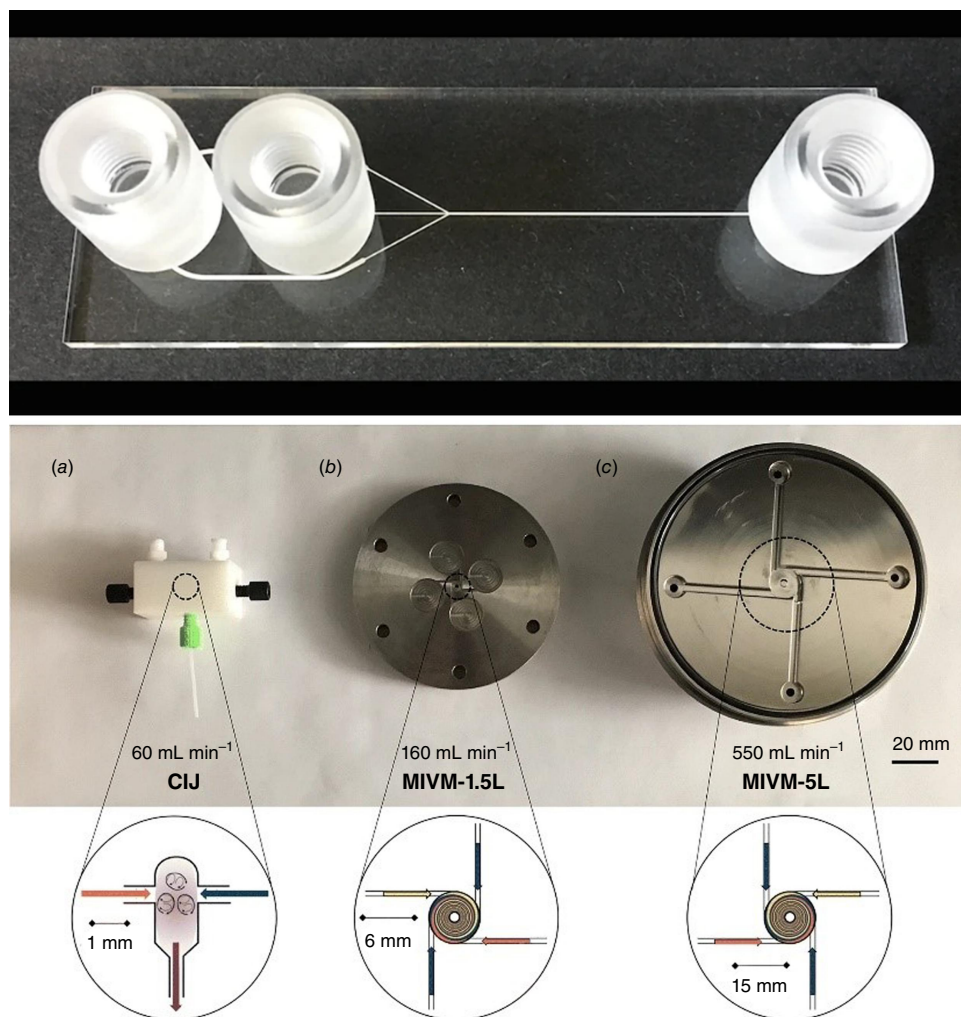


**Fig. 2.** Top: microfluidic devices as sold by Darwin Microfluidics, Herringbone Mixer – Glass Chip shown here; bottom: images of the three mixers: (a) confined impinging jet mixer (CIJ), (b) multi-inlet vortex mixer (MIVM)-1.5L, and (c) MIVM-5L, reproduced from Feng *et al.* (2019)<sup>32</sup> with permission from Springer Nature under Creative Commons CC BY.

or they can be assembled from simple parts. The sole driving force is the pressure applied by the pump that determines the mixing rate. The solutions are mixed by applying a range of geometries, with Y- or T-shaped inlets the simplest designs (Fig. 4). The two solutions then mix at the interface. A way of increasing the size of this interface is hydrodynamic flow focusing (HFF) where the central jet has higher velocities than the sheathing fluid.<sup>36</sup>

### From laminar flow to turbulent flow

As the channels in which the two solutions are combined are narrow, laminar flow is usually observed. Laminar flow occurs when the two solutions flow in parallel without

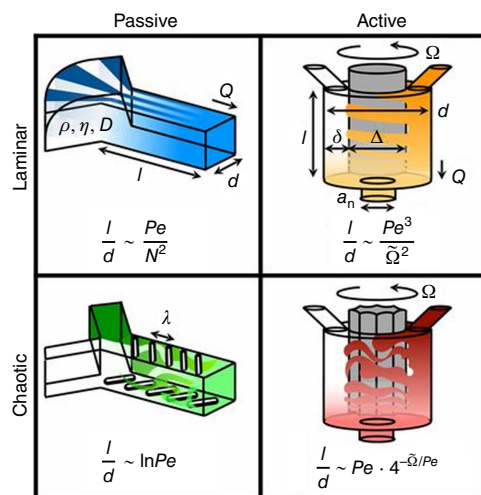


**Fig. 3.** Active and passive mixing with either laminar or chaotic mixing. Reproduced from Ober et al. (2015)<sup>35</sup> with permission of PNAS. Pe, Péclet number;  $Q$ , net volumetric flow rate;  $\Omega$ , dimensionless rotation rate;  $l$ ,  $d$ ,  $\lambda$ ,  $\delta$ ,  $\Delta$ ,  $a_n$  are dimensions of the devices;  $\rho$ , density; and  $\eta$ , viscosity.



**Fig. 4.** Mixing of two solutions by: (a) T-junction, (b) Y-junction, (c) hydrodynamic flow focusing.

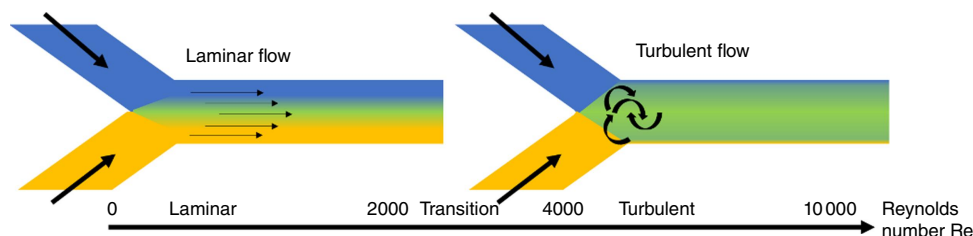


**Fig. 5.** Transition from laminar to turbulent mixing depending on the Reynolds number (Re).

disruption, which contrasts with turbulent flow where random fluctuations are observed during mixing. Whether the flow is laminar or turbulent can be predicated by the Reynolds number (Re), which is given by:

$$Re = \frac{\rho u L}{\mu}$$

where  $\rho$  is the density of the fluid ( $\text{kg m}^{-3}$ ),  $u$  is the flow speed ( $\text{m s}^{-1}$ ),  $L$  is the characteristic linear dimension (m) and  $\mu$  is the dynamic viscosity of the fluid ( $\text{kg m}^{-1} \text{s}^{-1}$ ). Laminar flow transitions into turbulent flow at Reynolds numbers approximately above 1800, well above the values obtained for parallel flow in a microfluidic device (Fig. 5).<sup>37</sup> Whether a device produces laminar or turbulent flow can be quickly observed by using two coloured solutions.<sup>38</sup>

The design of new microfluidic devices that enable faster mixing therefore became an integral part of this field. Passive micromixers that can create turbulent flows have built-in obstacles in the channels that create chaotic advection. This can be achieved by intersecting channels, zigzag channels, three-dimensional serpentine structures, channels with embedded barriers and slanted walls or twisted channels (Fig. 6).<sup>34</sup> Among all these devices, the staggered herringbone design has made a significant impact in this field over the last 20 years since it was first reported in 2002.<sup>39</sup> The V-shaped grooves, which are offset, cause transverse flow of the fluid, resulting in turbulent mixing (Fig. 7).<sup>40</sup> Since then, a range of devices have been developed, but the bifurcating mixer is highlighted here as it part of the NanoAssembl Platform that is widely used to assemble lipid nanoparticles.<sup>41</sup> This commercial assembly platform is now widely used in many research laboratories as its ease of operation allows even the non-expert to generate drug-loaded nanoparticles in a reproducible manner. The mixing chamber is based on the patented Dean Vortex Bifurcating Mixers (Fig. 6), which uses a design that resembles the bifurcating pattern produced by liquid jets discharging into a quiescent fluid.<sup>42</sup>

### Single-flow devices for the preparation of drug-loaded nanoparticles

Both laminar and turbulent approaches are used to prepared drug-loaded nanoparticles such as polyplexes. What all these flow-based assembly approaches have in common is fast and

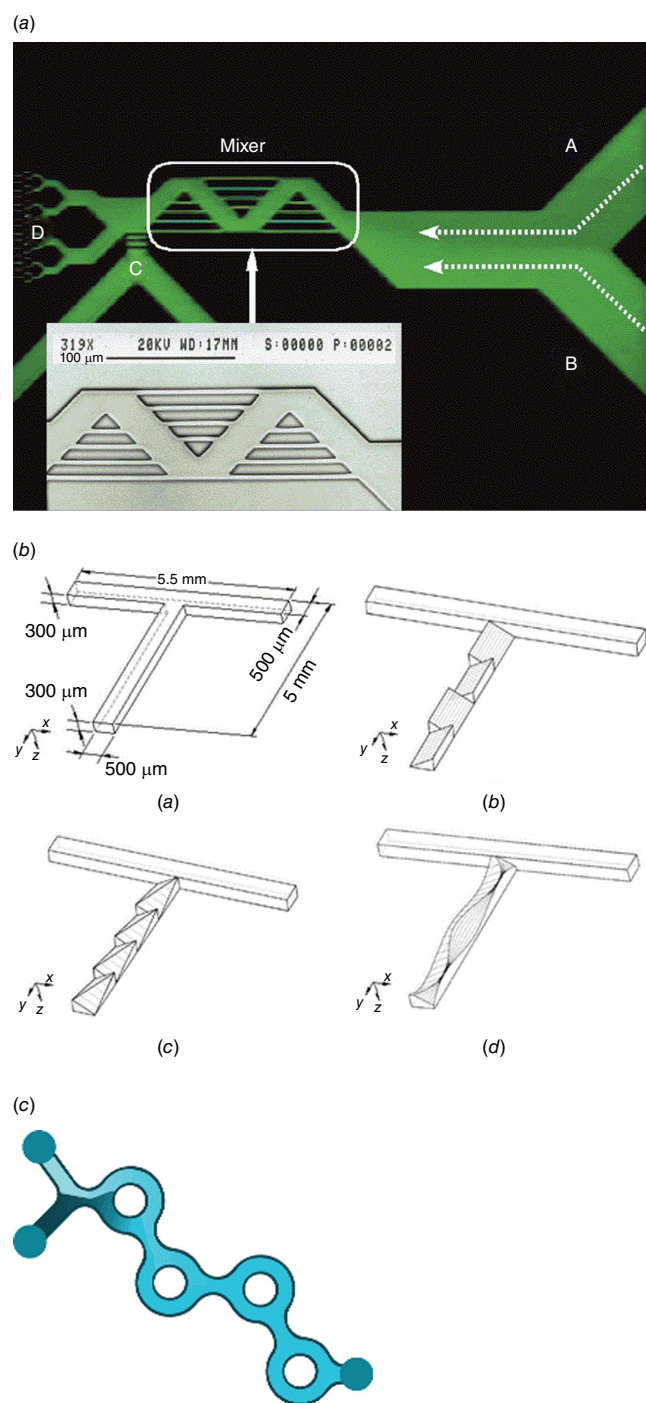


**Fig. 6.** (a) Photomicrograph and SEM of a microfluidic mixer with intersecting channels (A and B are entry channels, and C and D are outlet channels)<sup>43</sup>; (b) schematic diagrams (upside down) of (a) T-mixer, (b) inclined mixer, (c) oblique mixer, and (d) wavelike mixer.<sup>44</sup> Reproduced from Jen *et al.* (2003)<sup>44</sup> with permission of the Royal Society of Chemistry. (c) Dean Vortex bifurcating mixers as used in the NanoAssemblr Platform, reproduced with permission from Precision Nanosystems.

continuous mixing on the nanoscale and the elimination of a concentration gradient as depicted in Fig. 1. Many devices have been developed to generate reliable nanoparticles for drug delivery and the choice of device depends on the specific drug loading process. Polyplexes are usually prepared by mixing an aqueous solution containing the cationic polymer with the aqueous nucleic acid solution. The ratio between both components such as the nitrogen-to-phosphorus (N/P) ratio, concentration, flow rate and many more parameters determine the outcome. The N/P ratio is especially important considering that nanoparticle formation is solely based on electrostatic interactions between both ingredients. Once formed, the polyplex size is locked in unless strong introduced competitive forces disrupt the interaction between the charges. Mixing using laminar flow relies on molecular diffusion, which can occasionally be insufficient when trying to obtain narrow size distributions. However, laminar flow is still sufficient to generate better-defined nanoparticles than bulk mixing alone.<sup>38,46,47</sup> Sometimes, the nanoparticle size distribution is not improved compared with traditional preparation techniques to make polyplexes, but batch-to-batch variation is reduced, opening the door to large-scale production.<sup>48</sup> By contrast, turbulent mixing was found to generate polyplexes with high control. Among these techniques, the staggered herringbone mixer is widely used to generate nanoparticles loaded with drugs such as doxorubicin<sup>49</sup> or small interfering RNA (siRNA),<sup>50</sup> generating nanoparticle sizes with high precision and PDIs as low as 0.02.<sup>50</sup> The herringbone mixer enables the design of well-defined nanoparticles, but it does not shorten the optimisation workflow as each drug–drug carrier combination needs to be tested separately. To accelerate the process to identify suitable concentrations and, in the case of DNA delivery, suitable N/P ratios, a user-friendly microfluidic cartridge was prepared that can help screen seven N/P ratios in parallel (Fig. 7).<sup>45</sup> Here, several herringbone mixers are assembled on one chip, enabling the production of seven solutions with different N/P ratios in one process.

### Microfluidic-assisted nanoprecipitation (MF nanoprecipitation)

The formation of polyplexes based on water-soluble dendrimers and polymers is unique as, in contrast to other flow-based drug delivery approaches, no organic solvent is necessary. However, this only applies to soluble polymers and therefore excludes many degradable polymers such as polylactic acid (PLA). Nanoparticles based on hydrophobic polymers are in contrast prepared by mixing an organic solution containing the polymer and often the drug with an aqueous solution. Prerequisites are the miscibility of the organic solution and water and the immiscibility of the polymer in water. The relationship between these components is given by the ternary phase diagram of solute–solvent–non-solvent systems. When water is introduced into the system,

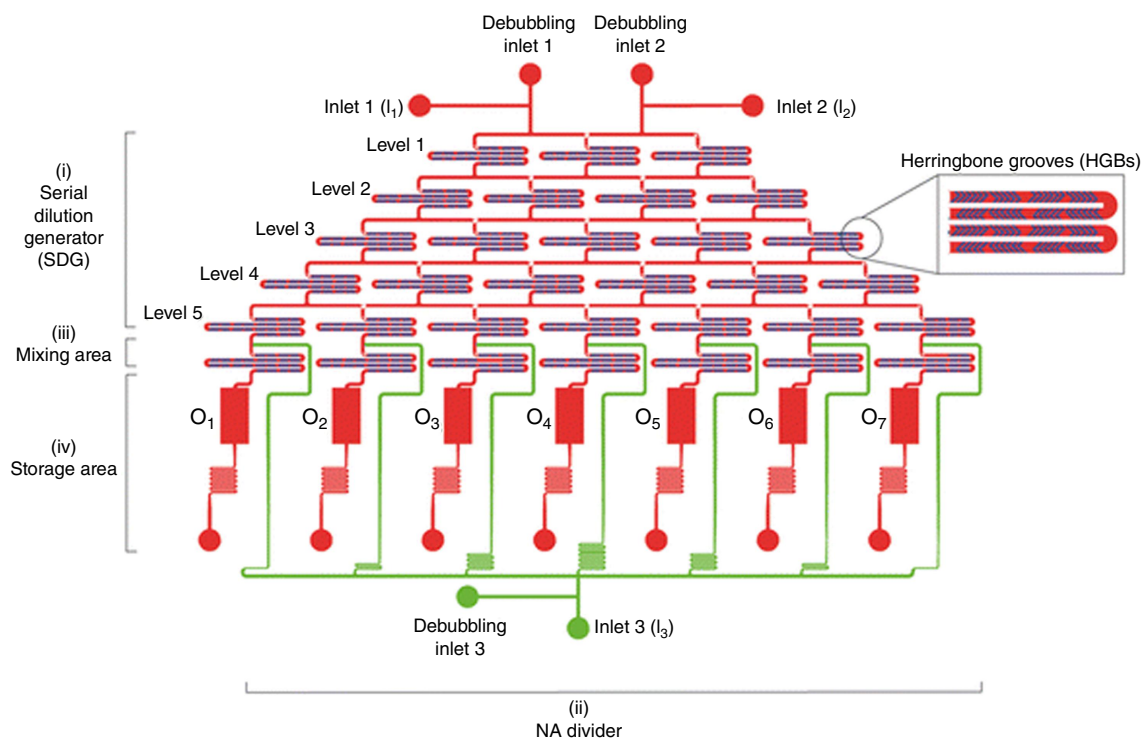


**Fig. 7.** The microfluidic cartridge consists of (i) an upstream five-level serial dilution generator (SDG) integrated with herringbone grooves (HGBs), (ii) a nucleic acid (NA) divider, (iii) a mixing area, and (iv) a storage area. The polymer solution and the water-based medium are injected into the two main inlets (inlets 1 and 2,  $I_1$  and  $I_2$ ) through the SDG and moved to the downstream area. An additional inlet ( $I_3$ ) allows for the addition and distribution of the DNA solution to the seven mixing units, where the polymer and DNA are mixed to give rise to polyplexes. These are collected in the storage tanks. Every inlet has a debubbling port. The middle right panel is a magnified view of the staggered HGB units integrated into the cartridge channels. Reproduced from Protopapa *et al.* (2023)<sup>45</sup> with permission of the Royal Society of Chemistry.

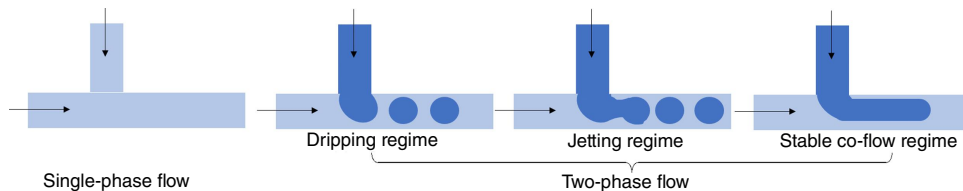


**Fig. 8.** Mode of mixing using either two miscible phase or droplets in a continuous phase.

the solubility of the polymer is reduced until at a specific water content, the binodal phase boundary is crossed, and thus nanoprecipitation occurs.<sup>51</sup> This process is heavily used on the laboratory scale where the organic solution is slowly dropped into excess water, but assembling these nanoparticles using flow can improve size distribution and size control. Flow-based devices range from HFF devices (Fig. 4)<sup>52</sup> and confined impinging jets mixers and to multi-inlet vortex mixers (Fig. 2).<sup>53,54</sup> The assembly process is not only affected by the flow device and parameters such as flow rate but also by the complex phase diagram, which is determined by the nature of the solvent and the type of polymer. Therefore, mixing-induced nanoprecipitation using flow is complex.<sup>51</sup> At the same time, the complexity opens the door to unusual nanostructured materials.<sup>51,55</sup>

## Segmented flow–multiphase system

Segmented-flow microfluidic systems use two immiscible fluids or a gas and fluid that can aid the mixing process.<sup>56</sup> With the addition of a new immiscible phase, droplets are formed that can assist the mixing process. Droplets are generated by an active method using valves or by a passive approach employing the inherent properties of the device and the solution. The droplet (dispersed) phase and the continuous phase can be combined from different direction such as by co-flowing, cross-flow (Fig. 8) or flow-focusing.<sup>57</sup> The viscosity of each liquid, the interfacial tension between both, the flow rate and the geometry of the inlet determine the subsequent steps. Fairly high surface instabilities are required to form droplets, which are typically present

when the interfacial tension  $\gamma$  is high, while viscosities  $\mu$  and flow rate  $u$  are small in relation.<sup>58</sup> This relationship is expressed by the dimensionless phase capillary number  $Ca = \mu \times u \div \gamma$  for the dispersed and the continuous phase, which can help to predict, among other influences, if droplets are formed or if the dispersed phase is not able to break up, resulting in the formation of jets (Fig. 8).<sup>58</sup> These droplets can potentially coalesce and the introduction of stabilisers such as polymers or surfactants are required.<sup>59</sup>

Liquid–liquid systems, often named emulsion-based or droplet-based microfluidic system, are widely employed to generate nanoparticles for drug delivery.<sup>59–61</sup> The size of the resulting nanoparticles is determined by the droplet size and can be predicted using the physical parameters of the system employed,<sup>58</sup> but in general, the nanoparticles tend to be above 100 nm in size.<sup>62</sup> The system is therefore useful to generate larger nanoparticles for nucleic acid delivery,<sup>63</sup> although it is possible to obtain small nanoparticles.<sup>64</sup> The clear advantage of this system is the ability to obtain non-spherical nanoparticles, but also the ability to create complex morphology when expanding the system from a two-phase to a multi-phase set-up.<sup>64</sup> Moreover, droplet-based microfluidics offer the opportunity to entrap nucleic acids into neutral hydrogels.<sup>65</sup> Whereas single-phase microfluidic systems rely on nanoprecipitation or electrostatic interaction paired with colloidal stabilisation to generate nanoparticles, the nature (size, shape) of the aqueous hydrogel droplets in droplet-based microfluidics is determined by the continuous organic phase. Droplet-based microfluidic systems, therefore, offer the opportunity to entrap these types of drugs in water-swollen polyethylene glycol (PEG) hydrogels.<sup>65</sup>

## Comparison of techniques

It is difficult to single out a technique that is superior to the others as this depends on various parameters. The first consideration is the type of polymer and drug and their solubility. As many polymers and drugs are not water-soluble, researchers need to identify a set-up that allows nanoprecipitation such as MF or flash nanoprecipitation. Hydrogel nanoparticles are in contrast better produced in multiphase systems.

Another aspect that influences the choice is the amount of nanoparticles that need to be prepared. Whereas a coaxial turbulent jet mixer can produce 3.15 kg of nanoparticles per day, single-channel microfluidic devices can only generate a few milligrams in the same timeframe.<sup>66</sup> However, this is often sufficient for further analysis in the development stage. The researcher might even prefer small-scale set-ups when trying to optimise the nanoparticle synthesis first.

Most important is, however, the knowledge and understanding required when choosing a system. Commercial assembly systems such as the NanoAssemblr Platform and other systems that are on the market are a great starting

point for researchers who have no knowledge of fluid dynamics. The former can easily be operated with a push of a button. However, these systems come with a price tag that may not be affordable for a laboratory. In such cases, researchers can choose from a range of commercially available microfluidic devices that can be easily assembled with syringe pumps or, if the budget permits, high-accuracy microfluidic pumps. As polydimethylsiloxane (PDMS)-based or glass-based channels are transparent, it is also possible to observe the flow with the help of a microscope. This can help with troubleshooting as well as identifying areas with precipitated product. Researchers with knowledge in fluid dynamics will most likely enjoy the design of new mixing channels that can achieve better outcomes.

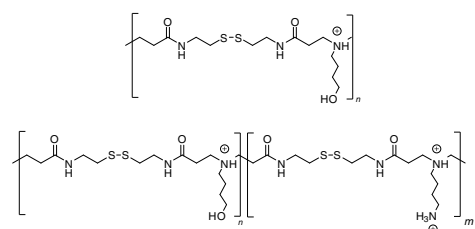
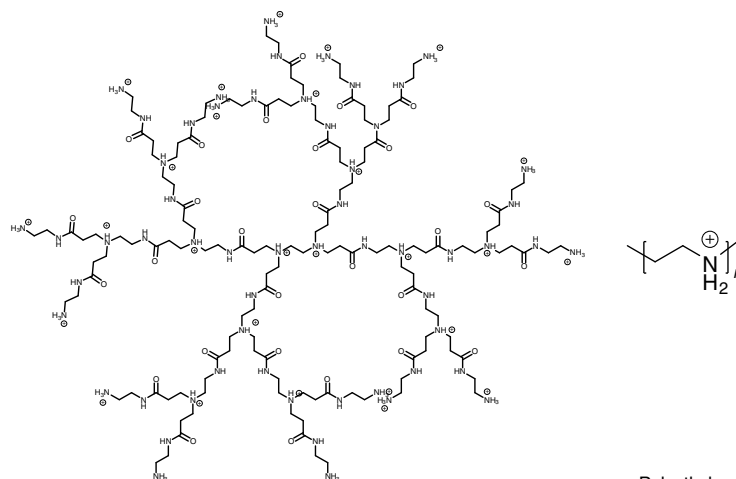
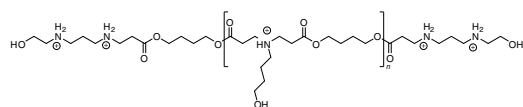
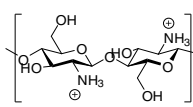
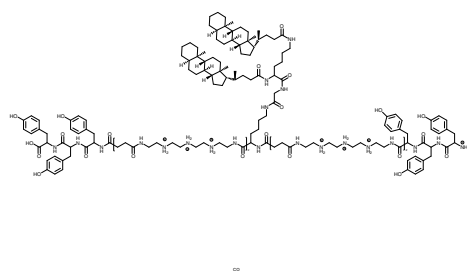
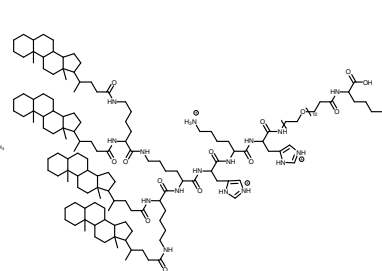
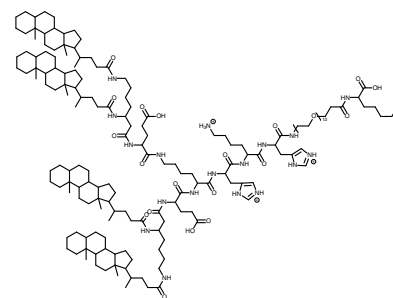
## Preparation of nanoparticles loaded with nucleic acid using flow

### Types of polymers employed to prepare DNA-based nanoparticles in flow

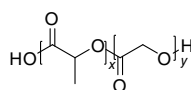
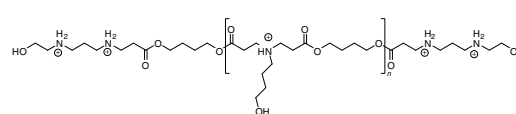
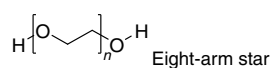
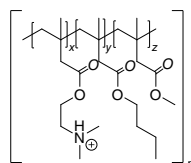
Flow-based assembly of nanoparticles has numerous benefits such as uniform mixing, ease of control and high efficiency,<sup>67</sup> resulting in good control in terms of dispersity, average particle size distribution and morphology.<sup>68,69</sup> Commonly, under bulk mixing conditions, polymers are dissolved in a solvent and then combined with another solution that contains the drug. Nanoparticle formation is then triggered by the formation of electrostatic interaction or by the addition of a non-solvent. The particle size, polydispersity and scaled-up production of nanoparticles may be affected by the mixing efficiency and time (Fig. 1). Although these issues apply to any nanoparticle synthesis, no other field is as much affected by heterogeneous mixing condition as the field of polymer nanoparticles. Polymers can easily be kinetically trapped, and strong forces between polymers and nucleic acid prevent the formation of nanoparticles that are in equilibrium with their environment. However, these characteristics can be controlled by microfluidics.<sup>70</sup> Many mixing technologies exist for nanoparticle preparation by flow as outlined above. This review, however, focuses on the preparation of polymer nanoparticles for nucleic acid delivery.

In general, there are two approaches to nucleic acid-loaded nanoparticles. Nanoparticles are either formed by compacting cationic polymers with nucleic acid to form polyplexes or by entrapping the negatively charged load into neutral, often hydrophobic polymers, usually with the help of a cationic polymers or cationic surfactant. Although many polymers have been explored for the delivery of nucleic acid,<sup>5</sup> the number of reports on flow-based assembly is limited (Fig. 9). In general, three different approaches have been explored: mixing of two aqueous solution containing polymer and nucleic acid respectively, nanoprecipitation and droplet-based microfluidics (Table 1).

## Cationic polymers

bioreducible poly(amido amine)s P(CBA-ABOL) and P(CBA-ABOL90/BDA10)<sup>66</sup>Polyamidoamine (PAMAM) dendrimer<sup>49</sup>Polyethylene imine (PEI)<sup>47,52</sup>Poly(beta-amino esters) (PBAE)<sup>48</sup>Chitosan<sup>73</sup>CO<sup>74</sup>LPO<sup>74</sup>LPOE<sup>74</sup>

## Neutral polymer mixed with cationic polymer

Poly(lactic-co-glycolic acid) (PLGA) and Eudragit<sup>®</sup><sup>75</sup>Eight-arm-PEG-mercapto-norbornene and eight-arm-PEG-mercaptoacetic acid and poly(beta-amino esters) PBAE<sup>67</sup>

## Neutral polymer mixed with cationic surfactants

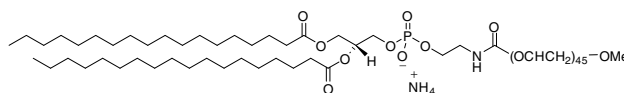
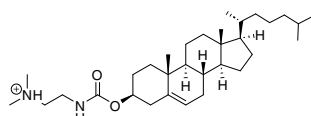
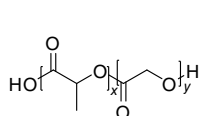
poly(lactic-co-glycolic acid) (PLGA)  
3β-[N,N'-dimethylaminoethane]-carbamoyl] cholesterol hydrochloride (DC-Cholesterol) (cationic)  
Methoxy-polyethylene glycol-1,2-distearoyl-sn-Glycero-3-phosphoethanolamine (mPEG2000-DSPE)<sup>76</sup>

Fig. 9. (Caption on next page)

**Fig. 9.** Polymers used for the preparation of nucleic acid-loaded nanoparticles using flow assembly; the cationic charges shown are dependent on the pH value (CO, LPO and LPOE are abbreviations given by Loy *et al.*<sup>71</sup> as core oligomer, lipid anchored PEG 12 oligomer, and lipid anchored PEG 12 oligomer without glutamic acid respectively).

### Assembly of water-soluble systems

The simplest is the assembly of polyplexes, which are made using cationic polymers and nucleic acids. The nanoparticles are then formed as a result of electrostatic binding,<sup>75</sup> which can be controlled by ionic strength and pH value, but also the nature of the cationic polymer.<sup>76,77</sup> Typical cationic polymers such as PEI, PAMAM dendrimer and chitosan were used to prepare polyplexes by flow, but some more unusual structures were also explored, as summarised in Fig. 9. This is, of course, a far cry from the myriad of cationic polymer structures that have already been tested for nucleic acid delivery and highlights that the field of flow assembly is only emerging.<sup>5</sup> The set-up appears fairly simple as two aqueous solutions are mixed either using turbulent flow such as in a microfluidic cartridge that contains herringbone grooves,<sup>45</sup> or by laminar flow in a microfluidic hydrodynamic focusing device,<sup>47</sup> which can have an advanced design and include single or double meandering channels.<sup>71</sup> The latter publication also discusses in detail the intricacies of flow assembly such as the pump pressure profile and the design of a system that can be used for scaling up. Here, the size of the final nanoparticles is the result of the chosen microfluidic set-up, type of polymer and payload, concentrations and flow rate (Re number). PAMAM dendrimers were mixed with siRNA using a funnel-shaped micromixer with several inlets. COMSOL Multiphysics software simulation suggested a laminar flow whose pattern changed depending on the flow rate.<sup>48</sup> (Fig. 9 and Table 1)

### Polymers for multiphase systems

Switching from a single phase to an emulsion system allows the design of PEG-based hydrogel nanoparticles that can be filled with PBAE-pDNA (Fig. 9) complexes. The size of the hydrogel particles that were prepared using eight-arms stars, crosslinked with thiol-ene chemistry, was determined by the set-up of the T-junction droplet break-up microfluidic device.<sup>65</sup> The resulting size of the aqueous PEG filled droplets was controlled by the channel dimensions and was adjusted between 41 and 142  $\mu\text{m}$ . Significantly smaller particles in the nanometre range were obtained when bioreducible poly(amido amine)s P(CBA-ABOL) and P(CBA-ABOL90/BDA10)<sup>63</sup> (Fig. 9 and Table 1) were loaded with mRNA and pDNA. The cationic polymer and the nucleic acid were directly mixed in the aqueous droplet.

### Polymers for nanoprecipitation

Additional components like neutral hydrophobic polymers, which are added to the mixture that contains cationic polymers and DNA, can help control size and stability and

therefore transfection efficiency. As soon as hydrophobic polymers are present, the use of organic solvents is essential. Nanoparticles are then formed when the organic solution is mixed with an aqueous solution; thus, microfluidic-assisted nanoprecipitation is employed. Although the use of organic solvent is usually undesirable, it is outweighed by the advantages hydrophobic and biodegradable polyesters such as poly(lactic-co-glycolic) acid (PLGA), polycaprolactone (PCL) and PLA provide.<sup>78</sup> Microfluidic-assisted nanoprecipitation was used to form PLGA-Eudragit nanoparticles (Fig. 9 and Table 1). The PLGA-Eudragit polymers (hydrophobic PLGA polymer and cationic Eudragit polymer) were dissolved in acetone and mixed with water in the microfluidic chip to form a core with positive charge that was able to entrap DNA by electrostatic interactions.<sup>73</sup> As the resulting nanoparticles are hydrophobic and may have a tendency to aggregate, hydrophilic surfactants are added. This was achieved by introducing mPEG<sub>2000</sub>-DSPE into the aqueous phase (Fig. 9 and Table 1). In this study, PLGA was used as the hydrophobic polymer dissolved in the organic phase together with cationic DC-cholesterols. The two phases were mixed in a toroidal micromixer to form spherical DNA-loaded nanoparticles. The hydrophobic polymer and surfactant form the core while the amphiphilic mPEG<sub>2000</sub>-DSPE is inserted at the interface, with the PEG block providing steric stabilisation and water solubility. As the core is positively charged thanks to the presence of the cationic surfactant, DNA can be bound by electrostatic interaction. In the final nanoparticle, the PEG chains covered the DNA, which prevented particle aggregation.<sup>74</sup>

### Comparison of bulk mixing with flow mixing

In the laboratory, nucleic acid-loaded nanoparticles are usually prepared by bulk mixing where the aqueous solution containing the cationic polymers is added to the DNA-siRNA solution or vice versa. As discussed earlier, local heterogeneities often prevent the formation of well-defined nanoparticles with low dispersities while it is difficult to target a specific size (Fig. 1). Microfluidic techniques can improve the efficiency of mixing of these two solutions to produce DNA-siRNA-loaded nanoparticles of high quality compared with the bulk method (Table 1).<sup>79</sup> For example, using a chaotic serial dilution generator (SDG), which is a stand-alone microfluidic cartridge that was designed to control the features of nanoparticles, smaller sized PEI-DNA polyplexes (145 nm) with lower dispersities (PDI < 0.2) were obtained compared with bulk mixing (176 nm, PDI > 0.5 at N/P ratio of 40).<sup>45</sup> Using the same materials, Koh *et al.* employed a different microfluidic device, a stand-alone microfluidic cartridge (a chaotic SDG), to obtain

**Table I.** Summary of polymers used to prepare nucleic acid-loaded nanoparticles using flow devices.

Polymer	Drug	Technique	Flow mixing		Bulk mixing		Remarks	References
			Size (nm)	PDI	Size (nm)	PDI		
Cationic polymers								
PBAE	DNA	Mixing of aqueous solutions in flow focusing devices with pinch channel					No difference between MF and BM and no size data shown	Wilson et al. (2017) <sup>47</sup>
P(CBA-ABOL)	pDNA	Water droplets in fluorocarbon oil emulsion-based microfluidic system	100	0.15	166	0.34		Grigsby et al. (2013) <sup>63</sup>
	mRNA		113.1	0.18	222	0.32		
PEI	pDNA	Mixing of aqueous solutions in cartridge with seven chaotic serial dilution generator and dividers for variation of N/P ratios	98	0.1	196	>0.4	N/P ratio 50	Protopapa et al. (2023) <sup>45</sup>
PEI	pDNA	Mixing of aqueous solutions in microfluidic hydrodynamic focusing device	494		898		N/P ratio 3.3, PDI not reported	Koh et al. (2009) <sup>46</sup>
PAMAM dendrimer	siRNA	Mixing of aqueous solution using funnel-shaped micromixer	86	0.18	87	>0.20	N/P ratio 20	Agnoletti et al. (2017) <sup>48</sup>
CO + siRNA + LPO	siRNA	Mixing of aqueous solution in a single or a double meander channel microfluidic chip	114.7	0.14	416.2	0.71		Loy et al. (2021) <sup>71</sup>
CO + siRNA + LPOE	siRNA		141.9	0.23	128.2	0.47		
Chitosan	pDNA	Mixing of aqueous solutions in in-line mixing system (AIMS) consisting of Y-mixer and pinch valves	199	0.68	165	0.25		Naeini et al. (2017) <sup>72</sup>
	siRNA		48	0.15	98	0.21		
Cationic polymer and neutral polymers								
Eight-arm-PEG-norbornene and eight-arm-PEG-mercaptoacetic acid and poly( $\beta$ -amino esters) PBAE	pDNA	Water in oil T-junction droplet break-up microfluidic device	$41 \times 10^3$ – $142 \times 10^3$				Size of microspheres dependent on channel size	Deveza et al. (2015) <sup>65</sup>
PLGA and Eudragit	pDNA	Microfluidic-assisted nanoprecipitation	170	0.25	98	0.21		Zoqlam et al. (2021) <sup>73</sup>
Cationic surfactant and neutral polymer								
PLGA DC-cholesterol (cationic) mPEG <sub>2000</sub> -DSPE (surfactant)	pDNA	Microfluidic-assisted nanoprecipitation in toroidal micromixer	83	0.11	136	0.23		Santhanes et al. (2022) <sup>74</sup>

MF, mixing by microfluidics; BM, bulk mixing.

similar results. The sizes of the polyplexes were bigger compared with those using the technique by Protopapa *et al.*, but the flow assembly still led to smaller nanoparticles (494 nm) and lower PDIs than bulk mixing (898 nm).<sup>47</sup> Although both research teams observed the same size and PDI reduction in flow mixing compared with bulk mixing, the differences in reported nanoparticle size can be assigned to the N/P ratio used. The formation of better nanoparticles was also reported in the study by Loy *et al.*<sup>71</sup> who mixed the cationic oligomers CO, LPO and LPOE shown in Fig. 9 with siRNA (CO + siRNA + LPO and CO + siRNA + LPOE) using bulk mixing and two different microfluidic devices, a single meander channel microfluidic chip and a double meander channel microfluidic chip. The size and PDI of the two polyplexes assembled using flow (CO + siRNA + LPO 114.7 nm, PDI < 0.20 and CO + siRNA + LPOE 128.2 nm, PDI 0.468) are smaller than from bulk mixing (CO + siRNA + LPO 141.9 nm, PDI 0.23 and CO + siRNA + LPOE 416.2 nm, PDI > 0.2). This chosen microfluidic device was observed to be highly efficient to produce small sizes and uniform siRNA-loaded nanoparticles.<sup>71</sup>

However, improved outcome using flow assembly is not automatically guaranteed. Agnoletti *et al.* found that improvement compared with bulk mixing can be a matter of N/P ratio as well as flow ratios.<sup>48</sup> Polyplexes obtained from PAMAM and siRNA only led to better outcomes compared with bulk mixing when the ratio between the flow rates of the two inlets was adjusted.<sup>48</sup> Little size improvement was also reported using poly(beta-amino esters) (PBAE). Wilson *et al.* used a microfabricated PDMS-glass chip to generate nanoparticles, but they found little advancement in terms of size and PDI. However, the device allowed efficient scale up, good control over the assembly process and the ability to form nanoparticles that were stable under long-term storage.<sup>47</sup>

As mentioned in the previous section, nanoprecipitation is one of the most commonly used nanoparticle fabrication methods to reduce the size and PDI of the nanoparticles.<sup>80</sup> Santhanes *et al.* used microfluidic nanoprecipitation and succeeded in generating smaller nanoparticles (83 nm) with lower dispersities (PDI < 0.2) than using bulk mixing nanoprecipitation.<sup>74</sup> By contrast, Zoqlam *et al.* observed very different outcomes as the size and PDI of the nanoparticles generated using microfluidic nanoprecipitation were larger than with bulk mixing nanoprecipitation.<sup>73</sup> It is, however, not possible to compare the quality of the devices as the differences may stem potentially from the polymers employed as Zoqlam *et al.* used PEG-based surfactants, which can prevent particle aggregation and aid in the mixing process.

Choice of the right microfluidic device is, however, essential to generate good nanoparticles, as shown by the study by Naeini *et al.*<sup>72</sup> The authors developed an in-line mixing system (AIMS) that was improved over the course of the study. This system was used to compare chitosan-siRNA and chitosan-pDNA (Fig. 9) polyplex formation. Compared with

bulk mixing, flow mixing at high Reynolds numbers was found to be a powerful tool to minimise the size and PDI of the resulting nanoparticles while being able to scale up production. With increasing siRNA concentration, the size of the flow-assembled chitosan-siRNA increased from 40 to 60 nm while the PDI of the polyplexes remained below 0.2. This contrasts with large-sized polyplexes (from 99 to 179 nm) with broad size distributions that were the result of bulk mixing. Different results were obtained when pDNA was used to prepare chitosan-pDNA polyplexes as the bulk mixing yielded better sizes than the nanoparticles prepared using microfluidic devices, which was attributed to the large size of pDNA.<sup>72</sup>

### Effect of solution and flow changes

So far, it is apparent that smaller-sized polyplexes with smaller PDIs can be produced using microfluidic devices. However, there are additional elements that can affect the size and DPI of nanoparticles such as flow rate ratio, N/P ratio, the design of the microfluidic devices, the chemical structure of the polymer, the type of nucleic acid drug, concentration and so on. Thus, in this section, we discuss the influences on size and PDI of some of these factors.

#### Flow rate ratio and other parameters

First, microfluidic devices require different flow rates depending on the microfluidic mixer and the material and drug used. Another important parameter is the flow rate of each solution or the flow rate ratio, which is an expression of the relative rate of both flows.

Nucleic acid-containing polymer nanoparticles are often prepared using two aqueous solutions, one containing the drug, the other the water-soluble polymer (Table 1). However, occasionally hydrophobic polymers are involved and then the nanoparticles are often prepared by nanoprecipitation, which uses two different phases, aqueous and organic. The flow rate ratio is defined by the flow rate of the aqueous to the organic phase. For example, pDNA-loaded lipid-polymer nanoparticles were synthesised using flow rate ratios of 3:1 and 5:1 in a toroidal micromixer device. Smaller sizes, smaller PDIs and more stable nanoparticles were formed with lower flow rate ratios.<sup>74</sup> However, in some studies, the opposite was observed and the size of nanoparticles decreased with increasing flow rate ratio as it changed from 1:1 to 5:1.<sup>81,82</sup> This contradicting scenario may be caused by a combination of factors like differences in concentrations of the two different phases, which could affect the flow impedance as the viscosity is changed in the micromixer, but it should also be noted that in these studies, very different drug carriers and payloads were explored.<sup>83</sup>

The mixing process of two aqueous solutions is similarly affected by flow rate ratios. A specifically designed microfluidic device that can control the flow rate in the centre and outer inlet separately was used to assemble PAMAM

dendrimer–siRNA complexes in (*N*-2-hydroxyethylpiperazine-*N*-2-ethane sulfonic acid, HEPES) buffer at flow rate ratios (centre inlet flow rate to outer flow rate) varying from 1:10 to 1:2.5.<sup>48</sup> With increasing ratio, the size of the nanoparticles decreased, but the PDI increased, with the best nanoparticle being produced at a flow ratio of 1:5.

Other influential parameters are the channel design of the microfluidic device. For example, a T-junction droplet break up microfluidic device with input channel dimensions ranging from 50, 100, 150 to 200  $\mu\text{m}$ , was used to demonstrate how the size of the nanoparticles is directly related to the dimensions of the input channel.<sup>65</sup> Further, the Reynolds number  $Re$  is another powerful tool to control the flow regime in a microfluidic device.<sup>84</sup> In the flow device used by Naeini *et al.*, laminar flow was obtained when the  $Re$  number was below 2000, whereas a  $Re$  number above 4000 led to turbulent flow. A  $Re$  number between 2000 and 4000 represents a transitional flow regime between both laminar and turbulent flow (Fig. 8). With the help of an AIMS, the  $Re$  number could be dialled from 26 to 4000. With increasing  $Re$  number, the respective size and PDI of the size distribution of chitosan–siRNA and chitosan–pDNA polyplexes were observed to be reduced.<sup>72</sup>

### N/P ratio

The N/P ratio is the mole ratio of the amino groups (N in the cationic polymer) to the amount of phosphate groups (P) in the nucleic acid therapeutic.<sup>85</sup> The N/P ratio is often discussed when preparing polyplexes using an aqueous solution of cationic polymer and an aqueous DNA solution as the N/P ratio is known to affect the size and PDI of the nanoparticles. For example, Koh *et al.* mixed PEI with pDNA and observed that a higher N/P ratio of 6.7 led to smaller and more uniform polyplexes compared with an N/P ratio of 3.3.<sup>46</sup> Protopapa *et al.*, who used the same polymer–drug combination, developed a stand-alone microfluidic cartridge that contained seven output ports to test seven different N/P ratios (N/P = 0, 10, 20, 30, 40, 50 and 60) at the same time. Although higher N/P ratios usually leads to smaller sizes and lower PDIs, the authors observed an optimum at a N/P ratio of 50.<sup>45</sup>

### Concentration

As with bulk mixing, the concentration of the solution plays an important role. In this case, it is important to distinguish between the different approaches. Mixing two aqueous solutions that contain polymer and drug respectively to generate polyplexes as shown in Fig. 1 is affected differently to microfluidic-assisted nanoprecipitation or droplet-assisted microfluidics.

An in-line mixing system (AIMS) of two aqueous solutions containing cationic oligomers CO and siRNA or alternatively pDNA showed that concentration may, however, not always influence the outcome. Whereas siRNA as payload led to size increases from 40 to 60 nm, when the siRNA concentration

was increased from 0.1 to 0.4  $\text{mg mL}^{-1}$ , there was no equivalent effect when pDNA was loaded. Moreover, the size of the siRNA polyplexes across all concentrations was smaller than that for the pDNA polyplexes. As the larger pDNA diffuses more slowly than the small siRNA, polyplexes prepared using pDNA led to broader size distributions.<sup>42</sup>

When organic solvents and hydrophobic polymers are involved, as in the case of microfluidic-assisted nanoprecipitation, the concentrations of hydrophobic polymer influence the rate of precipitation. Furthermore, the ingredients added to the aqueous solution can be highly influential on the outcome. Different concentrations (0, 0.8, 3.4, 8.6, 17.2  $\mu\text{g mL}^{-1}$ ) of pDNA dissolved in water together with the surfactant mPEG2000-DSPE were formulated with PLGA and cationic lipid DC-cholesterol that were both dissolved in organic solvent. With increasing concentration of pDNA, the size of the resulting nanoparticles decreased. The concentration of the surfactant has a similar effect as higher amounts lead to smaller sizes at higher flow rate ratios. However, at lower flow ratios, the system became unstable as evidenced by an increase in PDI.<sup>74</sup>

### Nature of polymer and drug

The nature of the polymer itself is a determining factor in the quality of the nanoparticles. Although there are plenty of studies on the relationship between polymer structure and nanoparticle properties available that use bulk mixing, there is limited information so far on flow-based mixing. Comparison of two cationic oligomers, LPO and LPOE, that differ in the length of the PEG chain (Fig. 9) and their complex with siRNA (CO + siRNA + LPO and CO + siRNA + LPOE) revealed that longer PEG ligands promote the formation of larger nanoparticles with larger PDIs.<sup>71</sup> Also, the payload influences the outcome as shown when comparing chitosan complexes with siRNA or pDNA. Polyplexes based on siRNA had smaller sizes and smaller PDIs than pDNA at the same concentration and flow rate.<sup>72</sup>

### Perspective and conclusion

Flow-based assembly of nanoparticles has become an established technique in laboratories and in industry. Researchers can choose from a wide range of set-ups, either chip-based or capillary-based. The mode of mixing is crucial as laminar flow will result in different outcomes to turbulent flow. Flow-based assembly of drug-loaded nanoparticles has clear advantages, but some challenges should also be mentioned.<sup>37</sup> It is evident that the nanoparticle production is highly reproducible, with limited batch-to-batch variations. This allows efficient scaling up and the supply of high-quality nanoparticles for clinical applications. Flow production also leads to better-defined nanoparticles with narrower size distribution while the size can be tuned with the operating parameters. On the downside, it is not easy to switch

all laboratory operations to flow without considering a range of challenges. For example, although polydimethylsiloxane devices can be quite cheaply produced, the material is sensitive to organic solvents. Glass, silicon, or polytetrafluoroethylene are in contrast more robust, but more costly. There are also some costs involved to set up a flow laboratory as pumps can be quite pricey whereas bulk mixing requires only a pipette and a beaker. There are also more demands on the researcher as flow assembly requires more specialised skills and ideally an understanding of fluid flow. Having established one system may not be sufficient to meet the demands of the laboratory as each nanoparticle may require adjustment. One aspect that may also deter researchers from using flow is the minimum sample size, which could be an important aspect when trying to assemble costly nucleic acids in flow. Although researchers can assemble small volumes down to only a few microlitres in bulk mixing, even the smallest microfluidic devices require larger sample sizes, notwithstanding that with cheaper pumps that have a pressure ramp, there is always a fraction that needs to be discarded. It also needs to be considered that flow design is not timesaving *per se* and complex channel design is required to parallelise the process to allow testing of different parameters in one system. In general, chip design is still the biggest drawback as current chips have only a single purpose and they cannot be adjusted to suit other purposes.<sup>86</sup> In this case, modular systems that can be changed and adjusted offer more flexibility. However, the advantages of flow assembly certainly outweigh potential obstacles and flow assembly is therefore an essential tool that will help accelerate nanomedicine research.

## References

- Mitchell MJ, Billingsley MM, Haley RM, Wechsler ME, Peppas NA, Langer R. Engineering precision nanoparticles for drug delivery. *Nat Rev Drug Discov* 2021; 20: 101–124. doi:10.1038/s41573-020-0090-8
- Halwani AA. Development of pharmaceutical nanomedicines: from the bench to the market. *Pharmaceutics* 2022; 14: 106. doi:10.3390/pharmaceutics14010106
- Shan X, Gong X, Li J, Wen J, Li Y, Zhang Z. Current approaches of nanomedicines in the market and various stage of clinical translation. *Acta Pharm Sin B* 2022; 12: 3028–3048. doi:10.1016/j.apsb.2022.02.025
- Hou X, Zaks T, Langer R, Dong Y. Lipid nanoparticles for mRNA delivery. *Nat Rev Mater* 2021; 6: 1078–1094. doi:10.1038/s41578-021-00358-0
- Kumar R, Santa Chalarca CF, Bockman MR, Bruggen CV, Grimme CJ, Dalal RJ, *et al.* Polymeric delivery of therapeutic nucleic acids. *Chem Rev* 2021; 121: 11527–11652. doi:10.1021/acs.chemrev.0c00997
- Paunovska K, Loughrey D, Dahlman JE. Drug delivery systems for RNA therapeutics. *Nat Rev Genet* 2022; 23: 265–280. doi:10.1038/s41576-021-00439-4
- Zhang L, Nguyen TLU, Bernard J, Davis TP, Barner-Kowollik C, Stenzel MH. Shell-cross-linked micelles containing cationic polymers synthesized via the RAFT process: toward a more biocompatible gene delivery system. *Biomacromolecules* 2007; 8: 2890–2901. doi:10.1021/bm070370g
- Hui Y, Yi X, Hou F, Wibowo D, Zhang F, Zhao D, *et al.* Role of nanoparticle mechanical properties in cancer drug delivery. *ACS Nano* 2019; 13: 7410–7424. doi:10.1021/acs.nano.9b03924
- Donahue ND, Acar H, Wilhelm S. Concepts of nanoparticle cellular uptake, intracellular trafficking, and kinetics in nanomedicine. *Adv Drug Delivery Rev* 2019; 143: 68–96. doi:10.1016/j.addr.2019.04.008
- Stenzel MH. The trojan horse goes wild: the effect of drug loading on the behavior of nanoparticles. *Angew Chem Int Ed Engl* 2021; 60: 2202–2206. doi:10.1002/anie.202010934
- Hoshyar N, Gray S, Han H, Bao G. The effect of nanoparticle size on *in vivo* pharmacokinetics and cellular interaction. *Nanomed* 2016; 11: 673–692. doi:10.2217/nmm.16.5
- Choi CHJ, Zuckerman JE, Webster P, Davis ME. Targeting kidney mesangium by nanoparticles of defined size. *Proc Natl Acad Sci USA* 2011; 108: 6656–6661. doi:10.1073/pnas.1103573108
- Perrault SD, Walkey C, Jennings T, Fischer HC, Chan WCW. Mediating tumor targeting efficiency of nanoparticles through design. *Nano Lett* 2009; 9: 1909–1915. doi:10.1021/nl900031y
- Soo Choi H, Liu W, Misra P, Tanaka E, Zimmer JP, Itty Ipe B, *et al.* Renal clearance of quantum dots. *Nat Biotechnol* 2007; 25: 1165–1170. doi:10.1038/nbt1340
- Gustafson HH, Holt-Casper D, Grainger DW, Ghandehari H. Nanoparticle uptake: the phagocytosis problem. *Nano Today* 2015; 10: 487–510. doi:10.1016/j.nantod.2015.06.006
- Alexis F, Pridgen E, Molnar LK, Farokhzad OC. Factors affecting the clearance and biodistribution of polymeric nanoparticles. *Mol Pharmaceutics* 2008; 5: 505–515. doi:10.1021/mp800051m
- Blanco E, Shen H, Ferrari M. Principles of nanoparticle design for overcoming biological barriers to drug delivery. *Nat Biotechnol* 2015; 33: 941–951. doi:10.1038/nbt.3330
- Cabral H, Matsumoto Y, Mizuno K, Chen Q, Murakami M, Kimura M, *et al.* Accumulation of sub-100 nm polymeric micelles in poorly permeable tumours depends on size. *Nat Nanotechnol* 2011; 6: 815–823. doi:10.1038/nnano.2011.166
- Yu W, Liu R, Zhou Y, Gao H. Size-tunable strategies for a tumor targeted drug delivery system. *ACS Cent Sci* 2020; 6: 100–116. doi:10.1021/acscentsci.9b01139
- Ulkoski D, Scholz C. Impact of cationic charge density and pegylated poly(amino acid) tercopolymer architecture on their use as gene delivery vehicles. Part 2: DNA protection, stability, cytotoxicity, and transfection efficiency. *Macromol Biosci* 2018; 18: 1800109. doi:10.1002/mabi.201800109
- Bauer M, Tauhardt L, Lambermont-Thijs HML, Kempe K, Hoogenboom R, Schubert US, *et al.* Rethinking the impact of the protonable amine density on cationic polymers for gene delivery: a comparative study of partially hydrolyzed poly(2-ethyl-2-oxazoline)s and linear poly(ethylene imine)s. *Eur J Pharm Biopharm* 2018; 133: 112–121. doi:10.1016/j.ejpb.2018.10.003
- Jiang Y, Stenzel M. Drug delivery vehicles based on albumin-polymer conjugates. *Macromol Biosci* 2016; 16: 791–802. doi:10.1002/mabi.201500453
- Joshi N, Liu DL, Dickson KA, Marsh DJ, Ford CE, Stenzel MH. An organotypic model of high-grade serous ovarian cancer to test the anti-metastatic potential of ROR2 targeted polyion complex nanoparticles. *J Mater Chem B* 2021; 9: 9123–9135. doi:10.1039/D1TB01837J
- Jiang Y, Wong CK, Stenzel MH. An oligonucleotide transfection vector based on hsa and pdmaema conjugation: effect of polymer molecular weight on cell proliferation and on multicellular tumor spheroids. *Macromol Biosci* 2015; 15: 965–978. doi:10.1002/mabi.201500006
- Jiang Y, Lu H, Khine YY, Dag A, Stenzel MH. Polyion complex micelle based on albumin-polymer conjugates: multifunctional oligonucleotide transfection vectors for anticancer chemotherapeutics. *Biomacromolecules* 2014; 15: 4195–4205. doi:10.1021/bm501205x
- Đorđević S, Gonzalez MM, Conejos-Sánchez I, Carreira B, Pozzi S, Acúrcio RC, *et al.* Current hurdles to the translation of nanomedicines from bench to the clinic. *Deliv and Transl Res* 2022; 12: 500–525. doi:10.1007/s13346-021-01024-2
- Hirota S, de Ilarduya CT, Barron LG, Szoka Jr FC. Simple mixing device to reproducibly prepare cationic lipid-DNA complexes (lipoplexes). *Biotechniques* 1999; 27: 286–290.
- Maeki M, Kimura N, Sato Y, Harashima H, Tokeshi M. Advances in microfluidics for lipid nanoparticles and extracellular vesicles and

- applications in drug delivery systems. *Adv Drug Deliv Rev* 2018; 128: 84–100. doi:10.1016/j.addr.2018.03.008
- 29 Jung HN, Lee SY, Lee S, Youn H, Im HJ. Lipid nanoparticles for delivery of rna therapeutics: current status and the role of in vivo imaging. *Theranostics* 2022; 12: 7509–7531. doi:10.7150/thno.77259
- 30 Ahmadi S, Rabiee N, Bagherzadeh M, Karimi M. Chapter 8. Microfluidic devices for gene delivery systems. In: Hamblin MR, Karimi M, editors. *Biomedical applications of microfluidic devices*. Academic Press; 2021. pp. 187–208.
- 31 Johnson BK, Prud'homme RK. Flash nanoprecipitation of organic actives and block copolymers using a confined impinging jets mixer. *Aust J Chem* 2003; 56: 1021–1024. doi:10.1071/CH03115
- 32 Feng J, Markwalter CE, Tian C, Armstrong M, Prud'homme RK. Translational formulation of nanoparticle therapeutics from laboratory discovery to clinical scale. *J Transl Med* 2019; 17: 200. doi:10.1186/s12967-019-1945-9
- 33 Zhang H, Zhu Y, Shen Y. Microfluidics for cancer nanomedicine: from fabrication to evaluation. *Small* 2018; 14: 1800360. doi:10.1002/smll.201800360
- 34 Lee CY, Chang CL, Wang YN, Fu LM. Microfluidic mixing: a review. *Int J Mol Sci* 2011; 12: 3263–3287. doi:10.3390/ijms12053263
- 35 Ober TJ, Foresti D, Lewis JA. Active mixing of complex fluids at the microscale. *Proc Natl Acad Sci USA* 2015; 112: 12293–12298. doi:10.1073/pnas.1509224112
- 36 Lu M, Ozcelik A, Grigsby CL, Zhao Y, Guo F, Leong KW, et al. Microfluidic hydrodynamic focusing for synthesis of nanomaterials. *Nano Today* 2016; 11: 778–792. doi:10.1016/j.nantod.2016.10.006
- 37 Liu D, Zhang H, Fontana F, Hirvonen JT, Santos HA. Current developments and applications of microfluidic technology toward clinical translation of nanomedicines. *Adv Drug Deliv Rev* 2018; 128: 54–83. doi:10.1016/j.addr.2017.08.003
- 38 Debus H, Beck-Broichsitter M, Kissel T. Optimized preparation of PDNA/poly(ethylene imine) polyplexes using a microfluidic system. *Lab Chip* 2012; 12: 2498–2506. doi:10.1039/c2lc40176b
- 39 Stroock AD, Dertinger SKW, Ajdari A, Mezic' I, Stone HA, Whitesides GM. Chaotic mixer for microchannels. *Science* 2002; 295: 647–651. doi:10.1126/science.1066238
- 40 Williams MS, Longmuir KJ, Yager P. A practical guide to the staggered herringbone mixer. *Lab Chip* 2008; 8: 1121–1129. doi:10.1039/b802562b
- 41 Ali MS, Hooshmand N, El-Sayed M, Labouta HI. Microfluidics for development of lipid nanoparticles: paving the way for nucleic acids to the clinic. *ACS Appl Bio Mater* 2021; doi:10.1021/acsabm.1c00732
- 42 Reynolds WC, Parekh DE, Juvet PJD, Lee MJD. Bifurcating and blooming jets. *Ann Rev Fluid Mechanics* 2003; 35: 295–315. doi:10.1146/annurev.fluid.35.101101.161128
- 43 He B, Burke BJ, Zhang X, Zhang R, Regnier FE. A picoliter-volume mixer for microfluidic analytical systems. *Anal Chem* 2001; 73: 1942–1947. doi:10.1021/ac000850x
- 44 Jen C-P, Wu C-Y, Lin Y-C, Wu C-Y. Design and simulation of the micromixer with chaotic advection in twisted microchannels. *Lab Chip* 2003; 3: 77–81. doi:10.1039/b211091a
- 45 Protopapa G, Bono N, Visone R, D'Alessandro F, Rasponi M, Candiani G. A new microfluidic platform for the highly reproducible preparation of non-viral gene delivery complexes. *Lab Chip* 2023; 23: 136–145. doi:10.1039/D2LC00744D
- 46 Koh CG, Kang X, Xie Y, Fei Z, Guan J, Yu B, et al. Delivery of polyethylenimine/DNA complexes assembled in a microfluidics device. *Mol Pharmaceutics* 2009; 6: 1333–1342. doi:10.1021/mp900016q
- 47 Wilson DR, Mosenia A, Suprenant MP, Upadhy R, Routkevitch D, Meyer RA, et al. Continuous microfluidic assembly of biodegradable poly(beta-amino ester)/DNA nanoparticles for enhanced gene delivery. *J Biomed Mater Res Part A* 2017; 105: 1813–1825. doi:10.1002/jbm.a.36033
- 48 Agnoletti M, Bohr A, Thanki K, Wan F, Zeng X, Boetker JP, et al. Inhalable siRNA-loaded nano-embedded microparticles engineered using microfluidics and spray drying. *Europ J Pharm Biopharm* 2017; 120: 9–21. doi:10.1016/j.ejpb.2017.08.001
- 49 Zhigaltsev IV, Belliveau N, Hafez I, Leung AKK, Huft J, Hansen C, et al. Bottom-up design and synthesis of limit size lipid nanoparticle systems with aqueous and triglyceride cores using millisecond microfluidic mixing. *Langmuir* 2012; 28: 3633–3640. doi:10.1021/la204833h
- 50 Belliveau NM, Huft J, Lin PJC, Chen S, Leung AKK, Leaver TJ, et al. Microfluidic synthesis of highly potent limit-size lipid nanoparticles for in vivo delivery of siRNA. *Mol Ther Nucleic Acids* 2012; 1: e37. doi:10.1038/mtna.2012.28
- 51 Chen T, Peng Y, Qiu M, Yi C, Xu Z. Recent advances in mixing-induced nanoprecipitation: from creating complex nanostructures to emerging applications beyond biomedicine. *Nanoscale* 2023; 15: 3594–3609. doi:10.1039/D3NR00280B
- 52 Karnik R, Gu F, Basto P, Cannizzaro C, Dean L, Kyei-Manu W, et al. Microfluidic platform for controlled synthesis of polymeric nanoparticles. *Nano Lett* 2008; 8: 2906–2912. doi:10.1021/nl801736q
- 53 Liu Y, Yang G, Zou D, Hui Y, Nigam K, Middelberg APJ, et al. Formulation of nanoparticles using mixing-induced nanoprecipitation for drug delivery. *Ind Eng Chem Res* 2020; 59: 4134–4149. doi:10.1021/acs.iecr.9b04747
- 54 Saad WS, Prud'homme RK. Principles of nanoparticle formation by flash nanoprecipitation. *Nano Today* 2016; 11: 212–227. doi:10.1016/j.nantod.2016.04.006
- 55 Yan X, Bernard J, Ganachaud F. Nanoprecipitation as a simple and straightforward process to create complex polymeric colloidal morphologies. *Adv Colloid Interface Sci* 2021; 294: 102474. doi:10.1016/j.cis.2021.102474
- 56 Ma J, Lee SM-Y, Yi C, Li C-W. Controllable synthesis of functional nanoparticles by microfluidic platforms for biomedical applications – a review. *Lab Chip* 2017; 17: 209–226. doi:10.1039/C6LC01049K
- 57 Glawdel T, Elbuku C, Ren CL. Droplet generation in microfluidics. In: Li D, editor. *Encyclopedia of microfluidics and nanofluidics*. Boston, MA, USA: Springer US; 2013. pp. 1–12.
- 58 Nunes JK, Tsai SSH, Wan J, Stone HA. Dripping and jetting in microfluidic multiphase flows applied to particle and fibre synthesis. *J Phys D: Appl Phys* 2013; 46: 114002. doi:10.1088/0022-3727/46/11/114002
- 59 Moragues T, Arguijo D, Beneyton T, Modavi C, Simutis K, Abate AR, et al. Droplet-based microfluidics. *Nat Rev Methods Primers* 2023; 3: 32. doi:10.1038/s43586-023-00212-3
- 60 Amirifar L, Besanjideh M, Nasiri R, Shamloo A, Nasrollahi F, de Barros NR, et al. Droplet-based microfluidics in biomedical applications. *Biofabrication* 2022; 14: 022001. doi:10.1088/1758-5090/ac39a9
- 61 Tian F, Cai L, Liu C, Sun J. Microfluidic technologies for nanoparticle formation. *Lab Chip* 2022; 22: 512–529. doi:10.1039/D1LC00812A
- 62 He F, Zhang M-J, Wang W, Cai Q-W, Su Y-Y, Liu Z, et al. Designable polymeric microparticles from droplet microfluidics for controlled drug release. *Adv Mater Technol* 2019; 4: 1800687. doi:10.1002/admt.201800687
- 63 Grigsby CL, Ho Y-P, Lin C, Engbersen JFJ, Leong KW. Microfluidic preparation of polymer-nucleic acid nanocomplexes improves nonviral gene transfer. *Sci Rep* 2013; 3: 3155. doi:10.1038/srep03155
- 64 Riahi R, Tamayol A, Shaegh SAM, Ghaemmaghami AM, Dokmeci MR, Khademhosseini A. Microfluidics for advanced drug delivery systems. *Curr Opin Chem Eng* 2015; 7: 101–112. doi:10.1016/j.coche.2014.12.001
- 65 Deveza L, Ashoken J, Castaneda G, Tong X, Keeney M, Han L-H, et al. Microfluidic synthesis of biodegradable polyethylene-glycol microspheres for controlled delivery of proteins and DNA nanoparticles. *ACS Biomater Sci Eng* 2015; 1: 157–165. doi:10.1021/ab500051v
- 66 Zhang L, Chen Q, Ma Y, Sun J. Microfluidic methods for fabrication and engineering of nanoparticle drug delivery systems. *ACS Appl Bio Mater* 2020; 3: 107–120. doi:10.1021/acsabm.9b00853
- 67 Luo G, Du L, Wang Y, Lu Y, Xu J. Controllable preparation of particles with microfluidics. *Particuology* 2011; 9: 545–558. doi:10.1016/j.partic.2011.06.004
- 68 Zhao C-X, He L, Qiao SZ, Middelberg APJ. Nanoparticle synthesis in microreactors. *Chem Eng Sci* 2011; 66: 1463–1479. doi:10.1016/j.ces.2010.08.039

- 69 Soni G, Yadav KS. Applications of nanoparticles in treatment and diagnosis of leukemia. *Mater Sci Eng C* 2015; 47: 156–164. doi:10.1016/j.msec.2014.10.043
- 70 Khan IU, Serra CA, Anton N, Vandamme TF. Production of nanoparticle drug delivery systems with microfluidics tools. *Expert Opin Drug Deliv* 2015; 12: 547–562. doi:10.1517/17425247.2015.974547
- 71 Loy DM, Krzysztoń R, Lächelt U, Rädler JO, Wagner E. Controlling nanoparticle formulation: a low-budget prototype for the automation of a microfluidic platform. *Processes* 2021; 9: 129. doi:10.3390/pr9010129
- 72 Tavakoli Naeini A, Soliman OY, Alameh MG, Lavertu M, Buschmann MD. Automated in-line mixing system for large scale production of chitosan-based polyplexes. *J Colloid Interface Sci* 2017; 500: 253–263. doi:10.1016/j.jcis.2017.04.013
- 73 Zoqlam R, Morris CJ, Akbar M, Alkilany AM, Hamdallah SI, Belton P, et al. Evaluation of the benefits of microfluidic-assisted preparation of polymeric nanoparticles for DNA delivery. *Mater Sci Eng C* 2021; 127: 112243. doi:10.1016/j.msec.2021.112243
- 74 Santhanes D, Wilkins A, Zhang H, John Aitken R, Liang M. Microfluidic formulation of lipid/polymer hybrid nanoparticles for plasmid DNA (pdna) delivery. *International J Pharm* 2022; 627: 122223. doi:10.1016/j.ijpharm.2022.122223
- 75 Ita K. Polyplexes for gene and nucleic acid delivery: progress and bottlenecks. *Eur J Pharm Sci* 2020; 150: 105358. doi:10.1016/j.ejps.2020.105358
- 76 Tros de Ilarduya C, Sun Y, Düzgüneş N. Gene delivery by lipoplexes and polyplexes. *Eur J Pharm Sci* 2010; 40: 159–170. doi:10.1016/j.ejps.2010.03.019
- 77 Elouahabi A, Ruyschaert J-M. Formation and intracellular trafficking of lipoplexes and polyplexes. *Mol Ther* 2005; 11: 336–347. doi:10.1016/j.ymthe.2004.12.006
- 78 Miladi K, Sfar S, Fessi H, Elaissari A. Nanoprecipitation process: from particle preparation to *in vivo* applications. In: Vauthier C, Ponchel G, editors. *Polymer nanoparticles for nanomedicines: a guide for their design, preparation and development*. Cham, Switzerland: Springer International Publishing; 2016. pp. 17–53.
- 79 Zhang L, Chen Q, Ma Y, Sun J. Microfluidic methods for fabrication and engineering of nanoparticle drug delivery systems. *ACS Appl Bio Mater* 2019; 3: 107–120. doi:10.1021/acsabm.9b00853
- 80 Brocchini S, James K, Tangpasuthadol V, Kohn J. A combinatorial approach for polymer design. *J Am Chem Soc* 1997; 119: 4553–4554. doi:10.1021/ja970389z
- 81 Roces CB, Christensen D, Perrie Y. Translating the fabrication of protein-loaded poly (lactic-co-glycolic acid) nanoparticles from bench to scale-independent production using microfluidics. *Drug Deliv Transl Res* 2020; 10: 582–593. doi:10.1007/s13346-019-00699-y
- 82 Kastner E, Kaur R, Lowry D, Moghaddam B, Wilkinson A, Perrie Y. High-throughput manufacturing of size-tuned liposomes by a new microfluidics method using enhanced statistical tools for characterization. *Int J Pharm* 2014; 477: 361–368. doi:10.1016/j.ijpharm.2014.10.030
- 83 Wild A, Leaver T, Taylor RJ. *Bifurcating mixers and methods of their use and manufacture*. Google Patents; 2018. US10076730B2. Available at <https://patents.google.com/patent/US10076730B2/en>
- 84 Green DW, Southard MZ. *Perry's chemical engineers' handbook*. McGraw-Hill Education; 2019.
- 85 Bono N, Ponti F, Mantovani D, Candiani G. Non-viral *in vitro* gene delivery: it is now time to set the bar! *Pharmaceutics* 2020; 12: 183. doi:10.3390/pharmaceutics12020183
- 86 Wu J, Fang H, Zhang J, Yan S. Modular microfluidics for life sciences. *J Nanobiotechnology* 2023; 21: 85. doi:10.1186/s12951-023-01846-x

**Data availability.** Any data are available from the authors.

**Conflicts of interest.** The authors declare that they have no conflicts of interest.

**Declaration of funding.** This research received funding from the Australian Research Council (ARC FL200100124) and the UNSW RNA Institute.

**Acknowledgements.** The authors thank the Australian Research Council and the UNSW RNA Institute for funding.

#### Author affiliations

<sup>A</sup>School of Chemistry, University of New South Wales, Sydney, NSW 2052, Australia.

<sup>B</sup>Children's Cancer Institute, Lowy Cancer Research Centre, University of New South Wales, Sydney, NSW 2052, Australia.

<sup>C</sup>School of Women's and Children's Health, University of New South Wales, Sydney, NSW 2052, Australia.

<sup>D</sup>UNSW RNA Institute, University of New South Wales, Sydney, NSW 2052, Australia.